Chapter 6

Poly-(lactic-co-glycolic-acid)-based particulate vaccines: nano-size is a key parameter for dendritic cell uptake and immune activation

Ana Luisa Silva*, Rodney A. Rosalia*, Eleni Varypataki,
Shanti Sibuea, Ferry Ossendorp & Wim Jiskoot

* Contributed equally to this study

Manuscript in preparation for publication

Abstract

Poly(lactide-co-glycolide) (PLGA) particulate vaccines have been extensively studied as delivery systems to improve the potency of protein based vaccines. In this study we analyzed how the size of PLGA particles, and hence their ability to be engulfed by dendritic cells, affects the type and magnitude of the immune response. PLGA microparticles (MP, volume mean diameter ≈ 112 μm) and nanoparticles (NP, Z-average diameter ≈ 350 nm) co-encapsulating ovalbumin (OVA) and poly(I:C), with comparable antigen (Ag) release characteristics, were prepared and characterized. NP were efficiently taken up by dendritic cells and induced MHC I Ag presentation *in vitro*, whereas MP failed to do so. Vaccination with NP resulted in significantly higher numbers of Ag-specific CD8+ T cells compared to MP and OVA emulsified with incomplete Freund's adjuvant (IFA). In addition, NP induced a balanced T_H1/T_H2-type antibody response, whereas MP failed to increase antibody titers and vaccinations with IFA led to a predominant T_H2-type response. In conclusion, we postulate that particulate vaccines should be formulated in the nano- but not micro-size range to achieve efficient uptake, significant MHC class I cross-presentation and improved T and B cell responses.

Introduction

In the past few years, extensive efforts in the field of cancer immunotherapy have led to the development of several therapeutic vaccine strategies currently being studied in clinical trials against various immunological diseases [1-3]. Protein- and peptide-based vaccines are popular forms of therapeutic vaccines [3-5] which have been tested succesfully in (pre-)clinical studies against various forms of cancer [6-8]. However, clinical benefits can still be significantly improved. Different methods can be applied to improve the efficacy of protein- or peptide-based vaccines, such as the combination with adjuvants, for example toll-like receptor ligands (TLRL), to enhance the otherwise poor immunogenicity of synthetic proteins and peptides [9,10]. In addition, optimizing the delivery of vaccines through the usage of biodegradable particles as vaccine carriers has resulted in promising results and significantly improved vaccine efficacy. Usage of biodegradable particles facilitates the co-delivery of a vaccine antigen (Ag) and TLR as one entity to dendritic cells (DC) [11,12].

DC are the most important and potent Ag-presenting cells (APC) of the immune system, scavenging the environment for potential pathogens [13,14]. DC have superior capacity to cross-present exogenous Ag in MHC I molecules and activate $CD8^+$ T cell responses. TLR-stimulation leads to DC maturation. Mature DC possess improved capacity to prime robust T cell response, essential for eradication of established tumors or clearance of pathogens. Therefore DC are considered the major target for cancer vaccines [15-17].

Montanide-based water-in-oil (w/o) emulsions are currently the main vaccine delivery systems used in the clinic. Montanide is a GMP-grade version of incomplete Freund's adjuvant (IFA). The Ag is dispersed in the emulsion which is injected subcutaneously (s.c.) or intradermal (i.d.) forming a local depot which slowly releases the emulsified Ag. Montanide (and) IFA have poorly defined adjuvant properties, but it is known to trigger inflammation at the injection site and immune cell infiltration [18,19]. However, the use of Montanide is associated with significant local adverse effects [6]. For these reasons, there is an urgent need for an alternative Ag delivery system [20].

Biodegradable particulate delivery systems are promising alternatives for Montanide [21]. Nanoparticles (NP) and microparticles (MP) prepared from poly(L-lactic-co-glycolic acid) (PLGA) have been studied extensively for the sustained delivery of proteins and therapeutic agents [22-24] Plain PLGA particles have sub-optimal adjuvant properties [10,25] but PLGA-particulate vaccines have shown potent anti-tumor effects by co-encapsulating tumor-associated Ag (TAA) and TH1-immunity promoting Toll like Receptor ligands (TLRL) [11,26,27].

Generally, particulate Ag (Ag) are better routed into MHC class I cross-presentation pathways, compared to soluble Ag, and therefore facilitate the priming of strong $CD8^+$ T cell responses.

It is generally assumed that NP, compared to MP, are ideal for (targeted) drug delivery due to better bio-distribution [28,29] and ability to cross biological barriers [30]. However, there is little agreement when it comes to vaccines for immunotherapy [31,32]. This may be related to different parameters that can direct the type and potency of the immune response, the target APC which the vaccine should be delivered to [33,34], efficiency of vaccine uptake by APC, Ag release kinetics and route of administration upon vaccination [35-38]. We have recently shown that low-burst release of the encapsulated Ag is critical for efficient MHC class I Ag presentation and $CD8^+$ T cell activation [39]. Accession of the MHC class I cross-presentation pathways was also shown to be dependent on particle size [40], however which size leads to the most efficient Ag cross-presentation remains debatable.

In this study, to compare the importance of particle uptake for the induction of an immune response, we developed NP and MP, formulated using PLGA, co-encapsulating the model Ag ovalbumin (OVA) and the TLR3L poly(I:C). NP can be internalized by DC [40], releasing the Ag inside endo-lysosomal compartments or directly inside the cytosol after uptake [41], versus MP which are poorly taken up by DC. MP most likely releases the encapsulated Ag in the extracellular matrix at the site of injection, similarly to Montanide. Formulated NP and MP contained equivalent amounts of Ag and TLRL and had comparable long-term Ag release profiles. We report here that NP are more efficiently internalized by DC *in vitro* and resulting in efficacious MHC class I cross-presentation and subsequent $CD8^+$ T cell activation *in vitro*. *In vivo*, NP showed superior vaccine potency compared to MP to stimulate cellular immune responses. In addition, NP out-performed water-in-mineral oil emulsion IFA as a vaccine carrier, more efficiently boosting $CD8^+$ T cell activation and (IgG2a) antibody production.

Materials and methods

Animals

WT C57BL/6 (CD45.2/Thy1.2; H-2^b) were obtained from Charles River Laboratories. Ly5.1/CD45.1 (C57BL/6 background) were bred in the specific pathogen-free animal facility of the Leiden University Medical Center. All animal experiments were approved by the animal experimental committee of Leiden University.

Reagents

PLGA Resomer RG 502H (50:50 MW 5,000–15,000 Da) was purchased from Boehringer Ingelheim (Ingelheim am Rhein, Germany) and PLGA Resomer RG 752H (75:25 MW 4,000-15,000 Da) was purchased from Sigma-Aldrich (Steinheim, Germany). Ovalbumin (OVA) grade V, 44 kDa was purchased from Worthington (LS003048) (New Jersey, USA). Alexa Fluor 488 labeled OVA was obtained from Invitrogen (Merelbeke, Belgium). Dichloromethane (DCM), dimethyl sulfoxide (DMSO), Hepes were purchased from Sigma–Aldrich (Steinheim, Germany). Tween 20 was purchased from Merck Schuchardt (Hohenbrunn, Germany) and polyvinyl alcohol (PVA) 4–88 (31 kDa) was purchased from Fluka (Steinheim, Germany). Poly(I:C) LMW and rhodamine labeled poly(I:C) were purchased from InvivoGen (San Diego, USA). Incomplete Freund adjuvant (IFA) was purchased from Difco Laboratories (Detroit, USA) Phosphate-buffered saline (NaCl 8.2 g/L; Na_2HPO_4.12 H_2O 3.1 g/L; NaH_2PO_4.2H_2O 0.3 g/L) (PBS) was purchased from B. Braun (Melsungen, Germany). All fluorescently labeled antibodies used for staining were purchased from BD Pharmingen (San Diego, USA) and the APC-SIINFEKL/H2-K^b tetramers were produced in house. All other chemicals were of analytical grade and all aqueous solutions were prepared with milli Q water.

IFA vaccine formulations were prepared by vortexing for 30 min a 1:1 IFA:PBS mixture. The vaccine-Ag was suspended in the PBS prior to addition to the IFA.

Cells

D1 cells, a GM-CSF dependent immature dendritic cell line derived from spleen of WT C57BL/6 (H-2^b) mice, were cultured as described previously [42]. Bone-marrow derived DC (BMDC) were freshly isolated from femurs from WT C57BL/6 strain and cultured as published previously [43]. After 10 days of culture, large numbers of cells were obtained which were at least 90% positive for murine DC marker CD11c (data not shown). B3Z $CD8^+$ T cell hybridoma cell line, specific for the H-2K^b-restricted $OVA_{257–264}$ CTL epitope SIINFEKL, expressing a β-galactosidase construct under the regulation of the NF-AT element from the IL-2 promoter, was cultured as described before [44]. OT-IIZ, a $CD4^+$ T-cell hybridoma cell line, specific for the I-A^b-restricted $OVA_{323–339}$ Th epitope, expressing the same β-galactosidase construct, was produced in house. The weakly immunogenic and highly aggressive OVA-transfected B16 tumor cell line (B16-OVA), syngeneic to the C57BL/6 strain, was cultured as described [45].

Preparation and characterization of OVA- and poly(I:C)-loaded PLGA particles

In this study, NP and MP were prepared containing the model Ag OVA and the TLR3 ligand poly(I:C). Plain PLGA-NP particles exhibit low immune activating properties [25] and are therefore poor vaccine-candidates. For this reason, all experiments were performed with particles co-encapsulating PolyI:C.

PLGA 50:50 and PLGA 75:25 NP were prepared by a water-in-oil-in-water (w/o/w) double emulsion with the solvent evaporation method as previously described [24]. The two types of PLGA, with different lactic acid:glycolic acid ratios (50:50 or 75:25 PLGA), influences hydrophobicity, polymer degradation rate and the release kinetics of OVA and poly(I:C).

In brief, 1 mg OVA (Worthington LS003048), 0.25 mg poly(I:C), were dissolved in 85 µl of 25 mM Hepes pH 7.4 and emulsified in 1 ml dichloromethane (DCM) containing 25 mg PLGA with an ultrasonic processor for 15 s at 20 W (Branson Instruments, CT, USA). A second emulsion was obtained by addition of 2 ml of 1% (w/v) PVA followed by sonication as described above. The double emulsion was added drop wise to 25 ml of an aqueous 0.3% PVA (w/v) solution at 40°C and the resulting mixture was stirred for 1 h. The resulting particles were harvested and washed twice with water by centrifugation (8000 *g*, 10 min).

PLGA 50:50 MP were prepared by adding 1 mg OVA, 0.25 mg poly(I:C) dissolved in 500 µl of 25 mM Hepes pH 7.4 to 1 ml DCM containing 125 mg PLGA 50:50. The mixture was emulsified with a homogenizer (30 sec) (max speed = 25,000 rpm) (Heidolph Ultrax 900, Sigma, Germany). The resulting emulsion was transferred to 10 ml of 2% (w/v) PVA and the 2nd emulsion was obtained by magnetic stirring (10 min, 750 rpm) at RT. Stirring was continues for 1 hr (500 rpm) (40°C) to allow evaporation of DCM. MP were harvested and washed with water twice by centrifugation (2000 *g*, 2 min). Particles ≥ 20 µm were separated via dia-filtration with 3 L water under continuous stirring in a Solvent Resistant Stirred Cell (Milipore, USA) filtration system with a 20 µm stainless steel metal sieve (Advantech, USA). The retentate was collected and MP recovered by centrifugation (2000 *g*, 2 min). MP larger than 200 µm were elimanated by using a 200 µm stainless steel metal sieve (Advantech, USA). The intactness of MP before and after filtration, were visualized with an Axioskop microscope (50 µl samples), equipped with an Axiocam ICc 5 (Carl Zeiss, Munich, Germany), using a 20x amplification objective. Images were collected using the ProgRes CapturePro v2.8.8 software (Jenoptik AG, Jena, Germany). Both NP and MP suspensions were aliquoted in cryovials and freeze-dried.

Alternatively, some particles were formulated with and 10 µg (10% w/w) OVA-Alexa488 and 1 µg (0.4%) poly(I:C)-rhodamine which were added to the inner emulsion for the preparation of NP and MP. This allowed quantification based on fluorescence and visualization by flow cytometry.

Mean size, size distribution and polydispersity index (PDI), obtained by dynamic light scattering (DLS) and Zeta potential (ZP) (applyting laser Doppler velocimetry) of NP were using a NanoSizer ZS (Malvern Instruments, Malvern, UK) at room temperature (RT) in 5 mM Hepes pH 7.4. The size distribution of MP was determined by light obscuration (LO) using a PAMAS SVSS system (PAMAS GmbH, Rutesheim, Germany) equipped with an HCB-LD-25/25 sensor and a 1-ml syringe. Results are averages of triplicate measurements, using runs, each of 0.2 ml (flow rate of 10 ml/min).

BCA assay (Pierce, Rockford, IL, USA) was used to determine OVA concentration in particles (before and after filtration) according to the manufacturer's instructions, after dissolving the particles in DMSO and 0.5 M NaOH + 0.5% SDS [46]. Encapsulation efficiency (EE) (see equation 6.1) of the protein was based on the OVA-Alexa-488 fluorescence (excitation 495 nm, emission 520 nm) and of TLR3L based on poly(I:C)-rhodamine (excitation 546 nm, emission 576 nm) detected in the supernatant using an Infinite® M 1000 Pro (Tecan, Switzerland) microplate reader. The drug loading (DL) was calculated according to equation 6.2. ("compound" stands for OVA or poly(I:C)):

$$\%\,\mathrm{EE} = \frac{\text{encapsulated compound mass}}{\text{initial compound mass}} \times 100 \qquad (6.1)$$

$$\%\,\mathrm{DL} = \frac{\text{encapsulated compound mass}}{\text{polymer mass} + \text{encapsulated compound mass}} \times 100 \qquad (6.2)$$

Microscopic analysis showed the quality and intactness of MP before filtration (BF) and after filtration (AF) (Figure 6.1). Physicochemical characterization of NP and MP is summarized in Table 6.1. NP were fairly monodisperse (PDI < 0.25), with NP 50:50 being 357 ± 25 nm and NP 75:25 being 400 ± 16 nm. The two different NP-formulations were produced with the aim to obtain NP of similar size but with varying release characteristics of the encapsulated protein. In addition, it was of importance to obtain NP with comparable Ag (and adjuvant)-release characteristics as MP for the purpose of studying the importance of size, while excluding other factors.

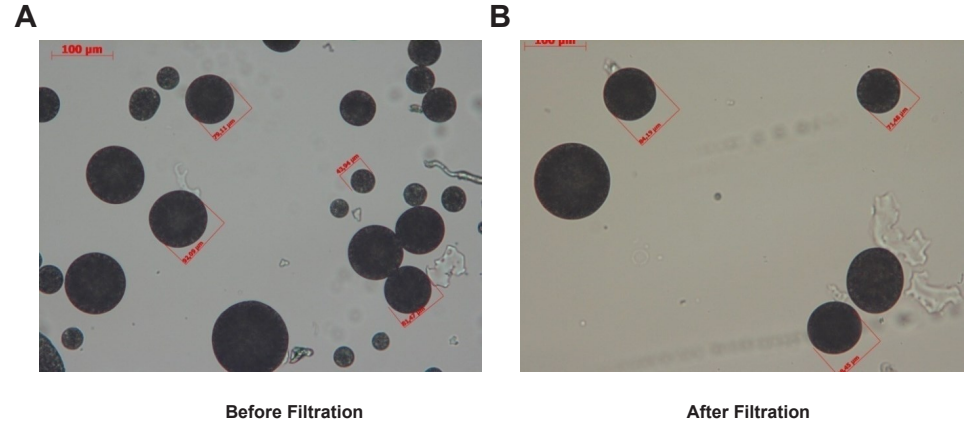

Figure 6.1 Representative images of MP preparations analyzed by optical microscopy (20x magnification) before and after stirred-cell filtration.

Table 6.1 Physical characteristics of OVA/poly(I:C)-loaded PLGA NP and MP*

Formulation	Size	PDI	ZP (mV)	OVA		Poly I:C	
				EE	DL	EE	DL
PLGA 50: 50# NP	357 ± 25 nm	0.16 ± 0.03	-41± 7	52 ± 7	2.01 ± 0.27	66 ± 8	0.63 ± 0.07
PLGA 75: 25# NP	400 ± 16 nm	0.25 ± 0.02	-25 ± 3	75 ± 1	2.87 ± 0.03	59 ± 7	0.56 ± 0.07
PLGA 50: 50# MP	17 ± 5 µm (n) 112 ± 26 µm (v)	n/a	-14 ± 3	86 ± 2	0.68 ± 0.01	81 ± 2	0.16 ± 0.00

*Values represent mean +/- standard deviation of 3 independently prepared batches .
#The two types of PLGA, with different lactic acid:glycolic acid ratios (50:50 or 75:25 PLGA), influences hydrophobicity, polymer degradation rate and the release kinetics of OVA and poly(I:C).
DL = drug loading; is a quantitative value for the ratio of protein:polymer; EE = encapsulation efficiency; is a qualitative value to define the efficiency of the formulation process to entrap the protein in the PLGA-polymer matrix = particles; PDI = poly dispersity index; variance, an arbitrary measure for the degree of dispersity in particle size within one batch of particles suspension, PDI values below 0.3 was considered monodisperse and accepted for follow up studies [47]; ZP = zeta potential; The magnitude of the zeta potential is predictive of the colloidal stability. Nanoparticles with Zeta Potential values greater than +25 mV or less than -25 mV typically have high degrees of stability. Dispersions with a low zeta potential value will eventually aggregate due to Van Der Waal inter-particle attractions.

For MP, size distribution, the average mean diameter based on volume Supporting Information Figure S6.1A and number Supporting Information Figure 6.1B before- and after filtration was determined.

The particle number-based mean diameter of MP, which is the average when considering the number distribution, increased from 5 ± 1 µm before filtration to 17 ± 5 µm after

filtration, showing that the filtration step effectively decreased the number of particles smaller than 20 µm, though not totally. However, the particle volume-based mean diameter was similar BF and AF (114 ± 16 vs 112 ± 26 µm) showing the relative minor contribution of small particles to the total particle volume. During the double-emulsion and solvent evaporation process, the OVA-protein added is equally distributed through the PLGA-polymer matrix and resulting particles. Thus the volume-based mean diameter results indicate that less than 1% of the total volume, and consequently the amount of the OVA added during formulation, corresponded to particles with diameters smaller than 20 µm after filtration (Supporting Information Table S6.1). Therefore, it is unlikely that residual NP after filtration would have a significant effect on Ag uptake, MHC class I Ag presentation and $CD8^+$ T cell activation, making them insignificant in terms of final immune response. Encapsulation efficiency of OVA (EE) was above 50% for all particle batches formulated with MP generally having higher EE% compared to NP. As explained above, the higher EE of OVA corresponds to the higher amount of PLGA content of MP compared to NP, which is reflected by the lower drug loading DL (Table 6.1). The use of different ratio of PLGA-polymer to formulate NP did not affect the EE of the protein nor the poly(I:C).

In vitro release studies

For release studies, PLGA particles (encapsulating 1% (w/w) of OVA-Alexa-488 and Poly(I:C)-rhodamine were resuspended in PBS/0.01% Tween-20/0.01% NaN_3 (pH 7.4) (10 mg PLGA/ml) at continous tangential shaking (100 rpm) at 37°C in a *GFL 1086* water bath (Burgwedel, Germany) for 30 days. At indicated time points, 250 µl samples of the suspension were taken, and centrifuged (18000x*g*) for 20 min and stored at 4°C until fluorescence intensity was determined as described above. Concentrations of OVA-Alexa-488 and poly(I:C)-rhodamine was assessed against a calibration curve. Release kinetics were based on fluorescence intensity because of the higher sensitivity achieved in comparison to the BCA assay. OVA content in the remaining supernatant (SN) on the last day of the release study were also analyzed using a BCA assay to compare to the results obtained using fluorescence measurements. The BCA assay and fluorescence assay showed comparable results (Supporting Information Table S6.2), justifying the use of fluorescence to assess OVA release from PLGA particles.

Release (R) profiles were generated in terms of cumulative release (%), as determined by equation 6.3, where "compound" is OVA or poly(I:C).

$$\%\,R = \frac{\text{compound mass in supernatant}}{\text{compound mass in supernatant} + \text{compound mass in particles}} \times 100 \qquad (6.3)$$

The OVA and poly(I:C) release kinetics were followed for 30 days. Release studies showed sustained release of OVA and poly(I:C) from PLGA 50:50 NP over this period (Figure 6.2A). Ag-release properties of MP were matched to those of NP by modifying the inner volume and salt content of the first emulsion during preparation of the MP (see Supporting Information Figure S6.2 for inner phase compositions).

OVA dissolved in 500 µl of 25 mM HEPES resulted in the fastest OVA release from MP (circa 40% OVA released after 15 days) comparable to that from NP (Figure 6.2C). The burst release of MP was decreased after filtration (AF) in comparison to MP analyzed before filtration (BF), most likely due to the elimination of the smaller MP (Supporting Information Figure S6.1 & Table 6.1). PLGA 75:25 NP (Figure 6.2B) showed release profiles resembling those of the MP. Thus, we formulated NP and MP using PLGA 50:50 with a similar composition but different Ag release properties; and NP using PLGA 75:25 with similar Ag-release profiles as PLGA 50:50 MP.

Ag release from particles appears to consist of an initial burst, followed by sustained release. After 30 days we observed a total release of 66 ± 6% OVA and 94 ± 7 poly(I:C) for NP 50:50, 51 ± 6% OVA and 64 ± 3 poly(I:C) for NP 75:25, and 44 ± 5% OVA and 54 ± 3 poly(I:C) for MP 50:50 (Figure 6.2).

In summary, we prepared NP and MP with similar long-term release characteristics, which will allow us to fairly compare the effects of particle size on in vitro DC uptake, MHC class I presentation and resulting *in vivo* immune activating properties.

Analysis of particle uptake by DC

Particle uptake by DC was determined by plating out D1 cells in 96-wells plate (10^5 cells/well) and pre-cooling the cells on on ice (10 min). Pre-cooled cells were then further cultured for 1 h at 4°C (on ice) or at 37°C in the presence of PLGA particles (PLGA-OVA/poly(I:C) NP/MP containing OVA-Alexa488) at the indicated concentrations. After incubation, cultured cells were washed and centrifuged twice with cold saline buffer to remove unbound particles and cells fixed with 4% paraformaldehyde (100 µl/well). Fixation was blocked by the addition of 100 µl/well fetal calf serum (FCS) and washing with cold PBS. From this point on cells were kept at RT and stained with rat anti-mouse CD45.2-APC fluorescent

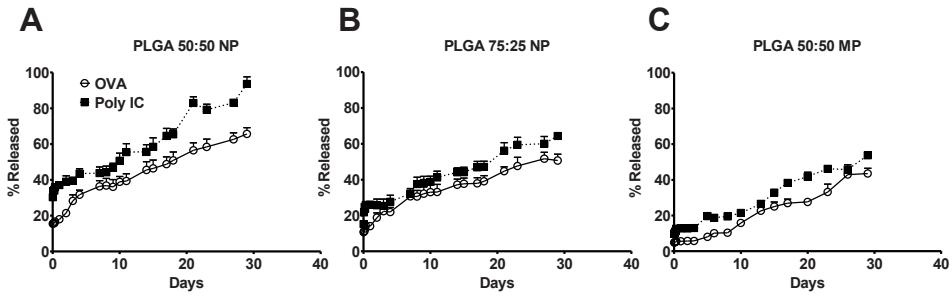

Figure 6.2 ***In vitro*** **release kinetics of OVA and poly(I:C) from NP and MP.**
OVA and poly(I:C) release in PBS/0.01% Tween-20/0.01% NaN_3 (pH 7.4) of **(A)** NP PLGA 50:50, **(B)** NP PLGA 75:25, and **(C)** MP PLGA 50:50 were monitored for 30 days at 37°C. Data are presented as average ± SD of 3 independent batches.

antibodies to allow detection of cells which were positive for particle association, based on OVA-Alexa488 fluorescence as analyzed using a BD LSRII flow cytometer. Samples were acquired using the BD FACS DIVA software and analyzed with Flow Jo software (treestar).

MHC class I Ag presentation

DC were incubated for 2 hr with PLGA-OVA formulations at the indicated concentrations, washed and followed by an overnight incubation (37°C) in the presence of B3Z $CD8^+$ T cell hybridoma's to measure MHC class I presentation. A colorimetric assay using chlorophenol red-β-D-galactopyranoside as substrate was used to detect IL-2 induced *lacZ* activity after recognition of SIINFEKL ($OVA_{257-264}$) in H-$2K^b$ by B3Z T cells [48]. To determine the relative maximum B3Z T cell activation DC were loaded with the minimal epitope SIINFEKL and the extinction value set as 100% (OD_{590nm} = 2.53 = 100% = maximal $CD8^+$ T cell activation).

Vaccination studies

Animals were vaccinated with the various PLGA-OVA/poly(I:C) formulations, soluble OVA/poly(I:C) in PBS, or OVA/poly(I:C) emusified in IFA by s.c. injection into the right flank. Animals were vaccinated again on day 28 (boost). Priming of *in vivo* cytotoxic $CD8^+$ T cells was assessed seven days after the 1st vaccination or 14 days after the 2nd vaccination by transferring splenocytes prepared from congeneic Ly5.1 C57BL/6 animals which were pulsed with the SIINFEKL short peptide (OVA_8, vaccine specific target cells) or ASNENMETM

short peptide (FLU9, vaccine non-specific control target cells). The target cells were labeled with either 10 µM (OVA) or 0.5 µM (Flu) CFSE. The cells were mixed 1:1 and 10^7 total cells were injected intravenously (i.v.) into the vaccinated animals. 18 hr post transfer of target cells, animals were sacrificed and single cell suspensions were prepared from isolated spleens. Injected target cells were distinguished by APC-conjugated rat anti-mouse CD45.1 mAb (BD Pharmingen, San Diego, USA). *In vivo* cytotoxicity was determined by flow cytometry as described above after 18 hr using equation 6.4:

$$\%\,\text{OVA - specific killing} = \left(1 - \left[\left(\frac{CFSE - peak\ area\ OVA}{CFSE - peak\ area\ FLU}\right)^{vaccinated\ animals} \times \left(\frac{CFSE - peak\ area\ OVA}{CFSE - peak\ area\ FLU}\right)^{non-vaccinated\ animals}\right]\right) \times 100 \qquad (6.4)$$

OVA-specific $CD8^+$ T cells present in the spleens were analyzed by co-staining with APC-conjugated SIINFEKL/H2-K^b tetramers, AF-conjugated anti-mouse CD8α mAb and V500-conjugated rat anti-mouse CD3 mAb. Flow cytometry analysis was performed as described above.

Detection of antibody responses

Antibody responses were determined by collecting serum samples on day 21 after initial vaccination (1 week before 2nd vaccination) and on day 35 (1 week after 2nd vaccination). IgG1, IgG2a and IgG2b titers against OVA were determined by ELISA. In brief, high absorbent 96-wells (Nunc immunoplates) plates were coated with 5 µg/ml OVA in PBS and incubated with titrated serum samples in 10% FCS in PBS. The specific antibodies were detected using streptavidine conjugated rabbit anti-murine IgG1, IgG2a and IgG2b mAb, followed by addition of horse-radish-peroxidase conjugated biotin. 3,3′,5,5′-Tetramethylbenzidine (TMB) was used as a substrate and the color conversion was stopped after 10 min with 0.16 M H_2SO_4, which was then measured on a spectrophotometer by absorbance at 450 nm ($OD450_{nm}$). To determine immune polarization the IgG2a/IgG1 ratios were determined using $OD450_{nm}$ values determined at 1:100 dilution given that values applied were ≥ 2-fold $OD450_{nm}$ of the negative control (sera from non-immunized mice).

RESULTS

PLGA-particles in the nano-size range facilitate efficient internalization by DC compared to MP

Efficiency of particle association with DC was studied by culturing DC in the presence of the 3 different particle formulations at 4°C (binding) and 37°C (binding & internalization). DC showed very high capacity to bind and internalize NP compared to MP (Figure 6.3A). DC were incubated with various concentrations of protein Ag encapsulated in both sizes of particles and we observed consistently that both 50:50 and 75:25 PLGA-NP showed similar effects and were engulfed with higher efficacy than (PLGA 50:50) MP (Figure 6.3B & C).

Efficient MHC class I Ag presentation by DC incubated with NP

MHC class I Ag cross-presentation of encapsulated protein Ag in NP compared to MP by dendritic cells was studied *in vitro*. DC were incubated with titrated amounts of Ag formulations and specific antigen presentation was analyzed by OVA epitope (SIINFEKL)-specific T cells. DC loaded with NP 50:50 and 75:25 efficiently activated B3Z $CD8^+$ T cells (Figure 6.4). Normalized values in panel A were calculated based on the $OD590_{nm}$ values obtained using DC loaded with SIINFEKL cultured together with B3Z $CD8^+$ T cells ($OD590_{nm}$ = 2.53 = 100% = maximal $CD8^+$ T cell activation). In contrast, DC pulsed with MP 50:50 poorly stimulated B3Z $CD8^+$ T cells.

Effective *in vivo* priming of Ag-specific $CD8^+$ T cells by NP-encapsulated protein

The *in vitro* experiments showed that NP, in contrast to MP, are efficiently internalized by DC followed by processing of encapsulated protein Ag into the MHC class I processing pathways, resulting in strong activation of B3Z $CD8^+$ T cells. NP 50:50 and NP 75:25 showed similar effects. Moreover, NP 50:50 showed similar or $CD8^+$ T cell priming *in vivo* as NP 75:25 (data not shown). Therefore, NP 50:50 were used for comparative *in vivo* studies with MP 50:50 and classical IFA emulsions.

The *in vivo* vaccine potency of NP and MP formulations was analyzed in comparison to protein Ag and poly(I:C) solution emulsified in IFA. Animals were vaccinated and 7 days

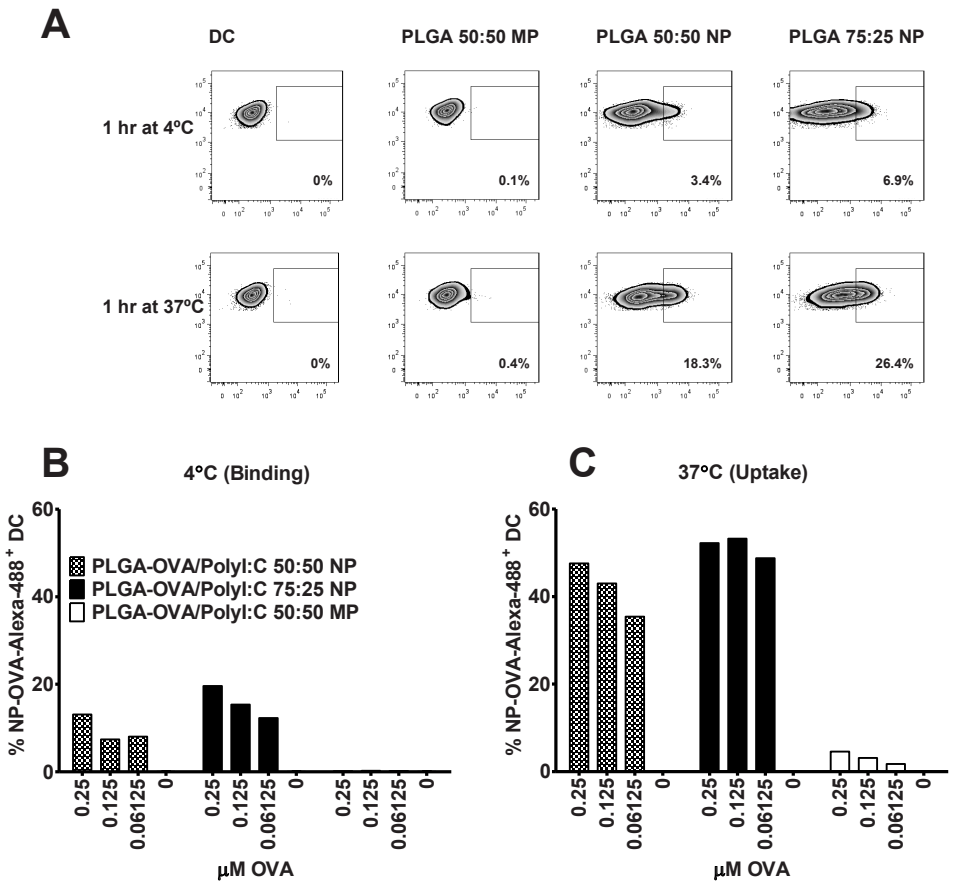

Figure 6.3 Binding and uptake of NP-encapsulated protein Ag by dendritic cells compared to MP-encapsulated Ag.

(A) D1 dendritic cells cells were incubated for 1 h with titrated amounts (μM) of OVA encapsulated in PLGA-NP (PLGA-OVA/poly(I:C) NP 50:50 or PLGA-OVA/poly(I:C) NP 75:25, or PLGA-MP PLGA-OVA/poly(I:C) MP 50:50 containing OVA-Alexa488 dye. Ag incubation with DC was performed in parallel at **(B)** 4°C (binding) and **(C)** 37°C (binding & internalization), followed by extensive washing to remove unbound Ag and cell fixation with 4% PFA. Cells were analyzed by flow cytometry to determine green fluorescence. Percentages of DC positive for OVA-Alexa-488 were quantified at different Ag concentrations. Data shown are measurements from one experiment.

later sacrificed to determine the number of primed endogenous Ag-specific $CD8^+$ T cells in the spleen (Figure 6.5). Vaccinations with NP 50:50 resulted in significantly higher numbers of SIINFEKL-TM^+ $CD8^+$ T cells compared to MP 50:50 ($P = 0.01$) and IFA ($P = 0.04$).

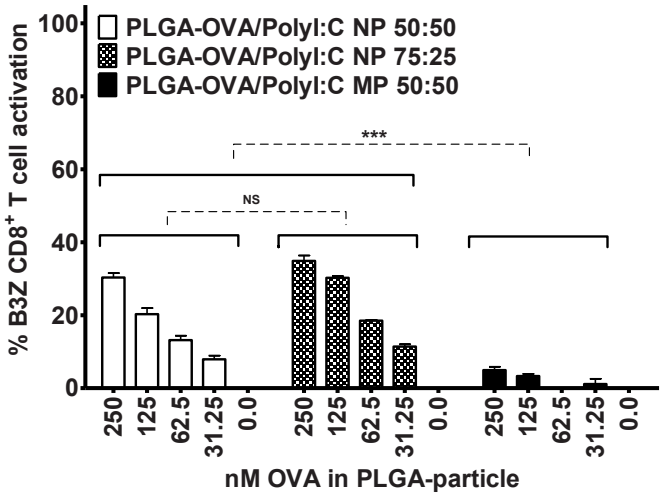

Figure 6.4 Efficient MHC class I cross-presentation of protein Ag incorporated in PLGA-NP but not PLGA-MP.

D1 cells were pulsed for 2 h with titrated amounts (μM) of OVA (and Poly(I:C) encapsulated in 50:50 PLGA-NP or 75:25 PLGA-NP or 50:50 PLGA-MP. MHC class I presentation of processed OVA protein antigen was detected by co-culture with H-2K^b/SIINFEKL-specific B3Z CD8$^+$ T cells. Data shown are means of triplicate measurements ± SD as % from one representative example out of at least three independent experiments.

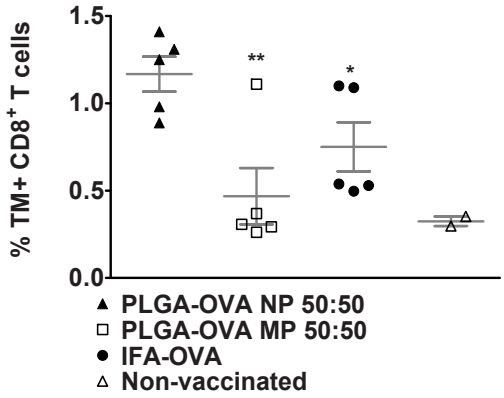

Figure 6.5 PLGA-OVA/poly(I:C) NP vaccine shows effective CD8$^+$ T cell priming potency.

Naïve animals received a single s.c. vaccination with the 50 μg OVA and 20 μg poly(I:C) formulated in particles or in IFA. Mice were sacrificed on day 7 after vaccination and the % of SIINFEKL-TM$^+$ CD8$^+$ T cells were measured by flow cytometry. Results shown are representative of one experiment out of two and present averages ± SEM from n = 3–5 mice per group, * = $P < 0.05$ & ** = $P < 0.01$ using an unpaired student t test. Each symbol represents the specific T cell response in an individual mouse.

PLGA NP efficiently prime CD8⁺ cytotoxic T cells which produce IFN-γ

Splenocytes of vaccinated mice were re-stimulated *ex vivo* with the minimal CD8⁺ T cell OVA epitope SIINFEKL. The cytokines IL-2 and IFN-γ were analyzed in the culture supernatants after 72 h (Figure 6.6). Significant amounts of IFN-γ were detected with the highest amounts produced by spleen cultures from animals vaccinated with NP 50:50 (Figure 6.6A) compared to the other vaccinated groups. However after one single vaccination, IL-2 production was barely above background levels (Figure 6.6B). Under these condition e also analyzed the CD8⁺ T cell *in vivo* cytotoxicity induced by vaccination with NP 50:50 compared to IFA-OVA/poly(I:C). In line with the relative higher number of specific CD8⁺ T cells induced with NP, we observed that animals vaccinated with NP 50:50 showed effective OVA-specific cytotoxicity to injected target cells *in vivo* (Supporting Information Figure S6.3).

Long term immune responses after a boost vaccination on day 28 were studied by analyzing *ex vivo* cytokine production on day 42. Using OVA-protein based vaccine formulations, poor overall production of IFN-γ was detected at this time point (Figure 6.6C). Notably, the 2nd

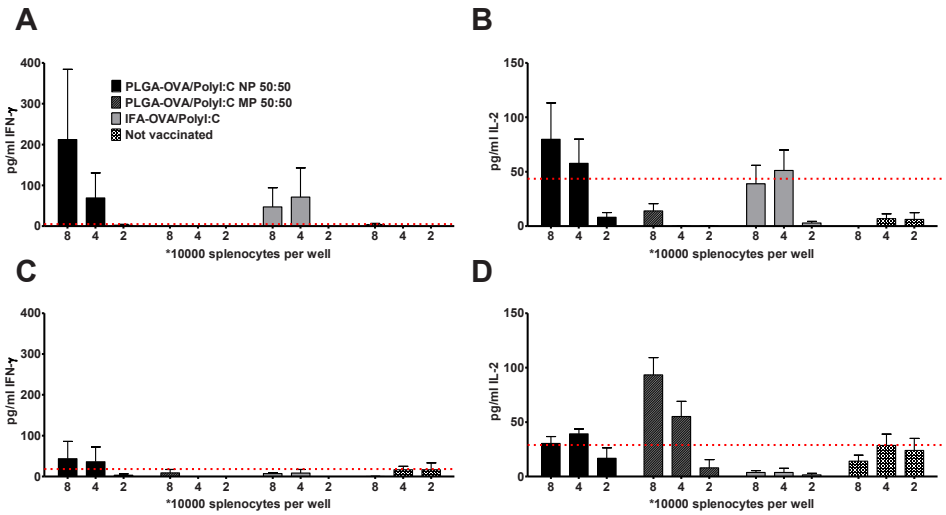

Figure 6.6 IFN-γ and IL-2 production after vaccination with PLGA-OVA/poly(I:C) NP. Animals were vaccinated with 50 µg OVA and 20 µg poly(I:C) formulated in particles or in IFA. Mice were sacrificed on day 7 post-vaccination, spleens harvested and single cell suspensions re-stimulated with 1 µM SSP-OVA_{8aa} (SIINFEKL). 72 h later the amount of Ag-specific **(A)** IFN-γ and **(B)** IL-2 produced determined by ELISA. Animals vaccinated twice (day 0 and 28) were sacrificed on day 42 and the *ex vivo* **(C)** IFN-γ and **(D)** IL-2 cytokine production analyzed 72 h later. Red dotted lines indicate average background production of cytokines in the absence of specific stimulation.

vaccination on day 28 resulted in higher levels of specific Ag-specific IL-2 production by splenocytes especially with MP 50:50 rather than the other groups (Figure 6.6D).

In conclusion, vaccination with NP resulted in the strongest production of IFN-γ compared to IFA or MP based vaccine formulations. NP did not induce strong production of IL-2 after a single vaccination nor double vaccinations. In contrast, MP were capable of inducing IL-2 production, but not IFN-γ, and only after the boost.

Ag-specific TH1 type humoral responses induced by vaccinations with PLGA-NP in contrast to IFA based vaccine

Blood samples were collected on day 21 or 35 after vaccinations. The titers of IgG1, IgG2a and IgG2b antibodies were determined as described in the section "materials & methods". NP 50:50 and IFA, but not MP, induced IgG1 production after one single vaccination (prime) (Figure 6.7A). Low titers of IgG2a and IgG2b were detected after NP and IFA vaccinations (Figure 6.7B & C). A second vaccination (boost) considerably enhanced the antibody titers. IFA and NP 50:50 led to the highest titers of IgG1, with MP formulations again failing to induce IgG1 titers (Figure 6.7D). Significant IgG2a titers were induced after a 2nd vaccination with NP 50:50 but poorly by the other vaccines (Figure 6.7E). IgG2b titers were induced to a similar level by vaccinations with IFA and NP 50:50 (Figure 6.7F). IgG2a is the IgG-subtype associated with T_H1 responses in mice. Analysis of the IgG1/IgG2a ratio allows one to determine the immune-polarization. Vaccinations with NP 50:50 resulted in a more balanced T_H1/T_H2 antibody response characterized by similar titers of IgG1 and IgG2a (IgG1/IgG2a ≈ 1). In contrast, vaccinations with IFA led to a predominant T_H2 response (IgG1/IgG2a > 2) (Figure 6.7G).

Discussion

Particulate vaccines are promising vaccine modalities to enhance immune activation. The immune system reacts more vigorously to vaccines presented in a particulate form compared to soluble ones [20,49,50]. However, the exact parameters needed to achieve robust immune responses using particulate vaccines are a matter of debate. Using PLGA particles co-encapsulating protein Ag and a TLR3L, we compared NP versus MP and studied the advantages of internalization of particles by DC to induce MHC class I cross-presentation *in vitro* and improve immune responses *in vivo*. We report here the importance to formulate

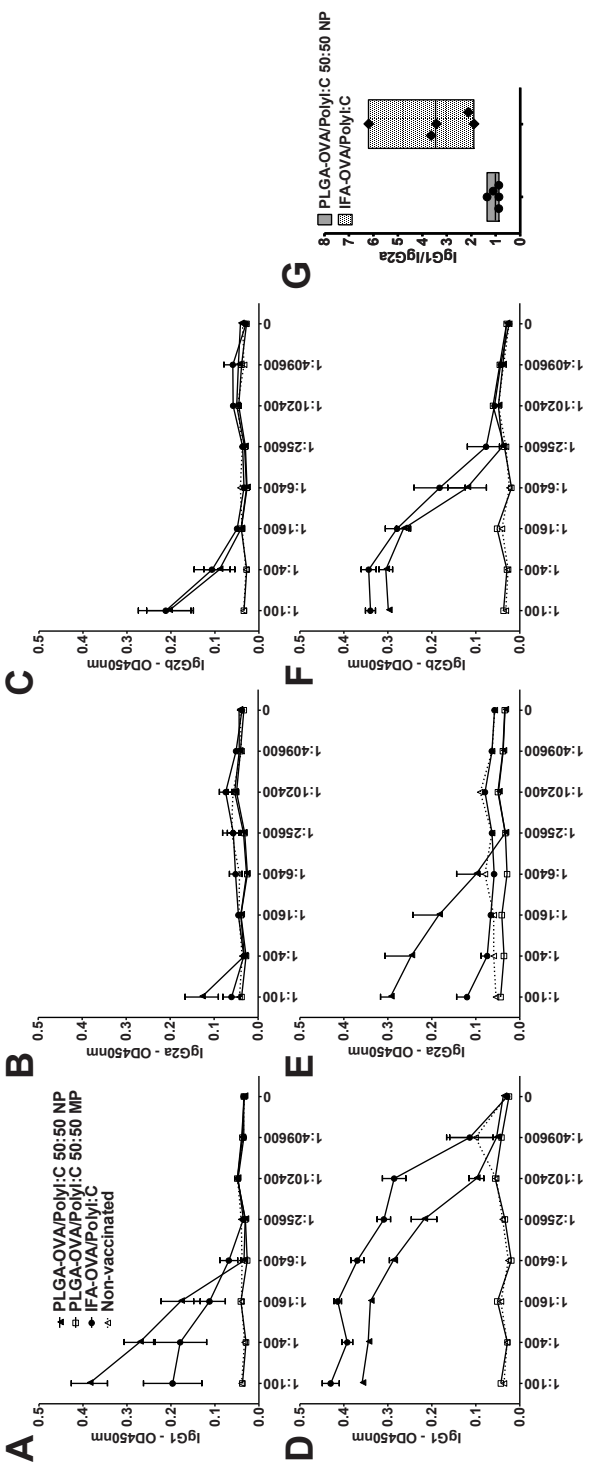

Figure 6.7 Induction of balanced TH1/TH2-associated humoral responses by vaccinations with PLGA-OVA/poly(I:C) NP.
(A) Animals were vaccinated on day 0 and day 28 with 50 µg OVA and 20 µg poly(I:C) formulated in particles or in IFA. Serum samples were collected on day 21 (3 weeks after prime, panel **A**, **B** and **C**) and 35 (1 week after boost, panel **D**, **E** and **F**) and the titers for IgG1, IgG2a and IgG2b determined via ELISA. **(G)** Immune polarization was calculated based on the IgG1/IgG2a ratio determining IgG1 ([$OD450_{nm}$ vaccinated mice/$OD450_{nm}$ non-immunize mice]/[IgG2a $OD450_{nm}$ vaccinated mice/$OD450_{nm}$ non-immunized mice]) at the lowest serum dilution (1:100). Results shown are averages ± SEM from 5 mice per group and time-point, * = $P < 0.05$, ** = $P < 0.01$ and *** = $P < 0.01$ two-way ANOVA with Bonferroni posttests.

nano-sized particles, to enhance MHC class I Ag-cross presentation and to improve both cellular and humoral immune responses.

Our observations are most probably associated with the fact that MP are poorly internalized as an whole entity cause of their large size. MP release the encapsulated via an initial burst followed by a more gradual escape of the Ag (Figure 6.2) due to the hydrolysis of the polymer. Therefore, MP basically deliver soluble Ag to DC. We and others have previously shown that DC poorly cross-present protein Ag when it's delivered in plain soluble form. Therefore, if the aim is to induce a robust $CD8^+$ T cell response through vaccination, MP might not be the right candidates for this purpose. Indeed, we observed very poor immune activation using MP as a vaccine carrier.

Our results argue against the application of MP as T cell vaccine carrier, however there exists some controversy in the literature regarding particle size and its importance for the formulation of efficient vaccine delivery systems and its effect on the activation of an immune response [37,38,51,52]. APC may take up and process Ag with similar dimensions to pathogens, from viruses, to bacteria, with the size influencing the mechanisms of uptake and processing by APC [53]. It has been reported that particles in the range of 20–200 nm are efficiently taken up by DC and facilitate the induction of cellular immune responses, whereas particles of 0.5–5 μm mainly generates humoral responses. There was limited uptake of 10 μm or larger particles leading to defective immune activation [32,36]. In contrast, others have reported that vaccinations with MP to also induce CTL responses, comparable to IFA or Montanide based delivery systems [20,54].

To study the effect of particle uptake on the subsequent immune response, NP and MP co-encapsulating OVA and poly(I:C) were required with similar Ag-release properties. Using the well-described double emulsion and solvent evaporation MP formulation technique [55], we at first obtained MP with very slow Ag-release properties (data not shown). Hence, the formulation process was modified and MP were engineered to accelerate release and to match the release properties of NP. For this purpose the inner emulsion volume and composition were modified to create a more porous matrix by adding salt to the inner water phase. Increasing the porosity accelerates drug diffusion and release from particles [56-59]. Replacing water with 25 mM Hepes pH 7.4 resulted in an increased Ag release rate from MP comparable to NP 75:25, respectively. TLRL always shows higher release rate than Ag, most likely due to its smaller size and more hydrophilic nature. NP are internalized by DC, whereas MP are not. We hypothesize that when administered *in vivo*, NP we formulated to

be taken up by APC as shown by others (Groettrup et al., JI 2012, Zhang et al., Biomaterials 2011), leading to sustained intracellular release [41,60].

MP were inferior to NP in facilitating MHC class I cross-presentation of encapsulated Ag with both NP 50:50 and NP 75:25 performing similarly, irrespective of release kinetics. Our observations are strengthened by the report of Joshi et al., who observed that efficiency of particle uptake and up regulation of MHC class I and CD86 expression on BMDC was dependent on particle size. However, considering the big differences in release kinetics observed, caution should be taken to conclude if there observations are indeed only dependent on the size and not caused by the considerable difference in Ag and TLRL release properties of the particles, since the initial (burst) release accounted for nearly all of the total Ag and or TLRL release.

Vaccinations with NP led to considerably higher numbers of Ag-specific $CD8^+$ T cells compared to MP ($P = 0.01$) and IFA ($P = 0.04$), with almost no difference being observed between vaccination with MP and non-vaccinated mice (Figure 6.5). NP also performed better than IFA, suggesting that internalization of the particles may be of importance in inducing a stronger cellular immune response in comparison to sustained release from a local Ag depot.

Though observing a substantial difference in burst release, the initial difference between NP and MP eventually attenuates over time, as MP slowly release Ag and TLRL into the extracellular matrix. Co-encapsulation of OVA and TLRL has previously shown to induce anti-OVA (IgG) humoral responses, as well as polarization of the immune response [36,61-63]. Vaccinations with NP 50:50 resulted in a more balanced T_H1/T_H2 antibody response characterized by similar titers of IgG1 and IgG2a ($IgG1/IgG2a \approx 1$). In contrast, vaccinations with IFA led to a predominant T_H2 response ($IgG1/IgG2a > 2$), which might contribute to the differences in $CD8^+$ T cell responses detected after vaccinations. A predominant humoral TH2 response will likely be accompanied by a weak $CD8^+$ T cell response. A balance between type 1 and type 2 responses is accompanied by robust $CD8^+$ T cell response induction in our NP system. The higher production of IgG2a after particle vaccination is linked to the increased uptake by DC of particles encapsulating the protein and adjuvant [64], compared to soluble protein and (most likely also) Poly(I:C). In addition, direct stimulation of B cells by the particles compared might also promote better IgG2a responses compared to IFA-based vaccine formulations [65,66].

In conclusion, our results show that the ability of a DC to internalize PLGA-particles is a crucial factor when aiming to achieve effective MHC class I presentation and to elicit an

immune response against encapsulated and processed Ag. Furthermore, because of the superior responses induced in comparison to IFA, our data support the application of biodegradable PLGA-NP delivery systems as a substitute for mineral oil emulsions for the delivery of protein vaccines for cancer immunotherapy.

Acknowledgements

The authors thank Ahmed Allam for the contribution to particle formulation studies. This study was supported by grants from Immune System Activation (ISA) Pharmaceuticals and the Leiden University Medical Center.

References

1. Ada G 2005. Overview of vaccines and vaccination. Mol Biotechnol 29:255-272.
2. Arens R, van HT, van der Burg SH, Ossendorp F, Melief CJ 2013. Prospects of combinatorial synthetic peptide vaccine-based immunotherapy against cancer. Semin Immunol.
3. Melief CJM 2008. Cancer Immunotherapy by Dendritic Cells. Immunity 29:372-383.
4. Waeckerle-Men Y, Allmen EU, Gander B, Scandella E, Schlosser E, Schmidtke G, Merkle HP, Groettrup M Encapsulation of proteins and peptides into biodegradable poly(D,L-lactide-co-glycolide) microspheres prolongs and enhances antigen presentation by human dendritic cells.
5. Zhang H, Hong H, Li D, Ma S, Di Y, Stoten A, Haig N, Di GK, Yu Z, Xu XN, McMichael A, Jiang S 2009. Comparing pooled peptides with intact protein for accessing cross-presentation pathways for protective CD8+ and CD4+ T cells. J Biol Chem 284:9184-9191.
6. Kenter GG, Welters MJ, Valentijn AR, Lowik MJ, Berends-van der Meer DM, Vloon AP, Essahsah F, Fathers LM, Offringa R, Drijfhout JW, Wafelman AR, Oostendorp J, Fleuren GJ, van der Burg SH, Melief CJ 2009. Vaccination against HPV-16 oncoproteins for vulvar intraepithelial neoplasia. N Engl J Med 361:1838-1847.
7. Atanackovic D, Altorki NK, Stockert E, Williamson B, Jungbluth AA, Ritter E, Santiago D, Ferrara CA, Matsuo M, Selvakumar A, Dupont B, Chen YT, Hoffman EW, Ritter G, Old LJ, Gnjatic S 2004. Vaccine-induced CD4+ T cell responses to MAGE-3 protein in lung cancer patients. J Immunol 172:3289-3296.
8. Sabbatini P, Tsuji T, Ferran L, Ritter E, Sedrak C, Tuballes K, Jungbluth AA, Ritter G, Aghajanian C, Bell-McGuinn K, Hensley ML, Konner J, Tew W, Spriggs DR, Hoffman EW, Venhaus R, Pan L, Salazar AM, Diefenbach CM, Old LJ, Gnjatic S 2012. Phase I trial of overlapping long peptides from a tumor self-antigen and poly-ICLC shows rapid induction of integrated immune response in ovarian cancer patients. Clin Cancer Res 18:6497-6508.
9. Celis E 2007. Toll-like Receptor Ligands Energize Peptide Vaccines through Multiple Paths. Cancer Research 67:7945-7947.
10. Kasturi SP, Skountzou I, Albrecht RA, Koutsonanos D, Hua T, Nakaya HI, Ravindran R, Stewart S, Alam M, Kwissa M, Villinger F, Murthy N, Steel J, Jacob J, Hogan RJ, Garcia-Sastre A, Compans R, Pulendran B 2011. Programming the magnitude and persistence of antibody responses with innate immunity. Nature 470:543-547.
11. Heit A, Schmitz F, Haas T, Busch DH, Wagner H Antigen co-encapsulated with adjuvants efficiently drive protective T cell immunity.
12. Schlosser E, Mueller M, Fischer S, Basta S, Busch DH, Gander B, Groettrup M 2008. TLR ligands and antigen need to be coencapsulated into the same biodegradable microsphere for the generation of potent cytotoxic T lymphocyte responses. Vaccine 26:1626-1637.
13. Banchereau J, Steinman RM 1998. Dendritic cells and the control of immunity. Nature 392:245-252.

14. Steinman RM 2001. Dendritic cells and the control of immunity: enhancing the efficiency of antigen presentation. Mt Sinai J Med 68:160-166.

15. Melief CJ 2008. Cancer immunotherapy by dendritic cells. Immunity 29:372-383.

16. Steinman RM 2012. Decisions about dendritic cells: past, present, and future. Annu Rev Immunol 30:1-22.

17. Tacken PJ, de Vries IJ, Torensma R, Figdor CG 2007. Dendritic-cell immunotherapy: from ex vivo loading to in vivo targeting. Nat Rev Immunol 7:790-802.

18. Vitoriano-Souza J, Moreira N, Teixeira-Carvalho A, Carneiro CM, Siqueira FA, Vieira PM, Giunchetti RC, Moura SA, Fujiwara RT, Melo MN, Reis AB 2012. Cell recruitment and cytokines in skin mice sensitized with the vaccine adjuvants: saponin, incomplete Freund's adjuvant, and monophosphoryl lipid A. PLoS One 7:e40745.

19. Harris RC, Chianese-Bullock KA, Petroni GR, Schaefer JT, Brill LB, Molhoek KR, Deacon DH, Patterson JW, Slingluff CL, Jr. 2012. The vaccine-site microenvironment induced by injection of incomplete Freund's adjuvant, with or without melanoma peptides. J Immunother 35:78-88.

20. Mueller M, Schlosser E, Gander B, Groettrup M 2011. Tumor eradication by immunotherapy with biodegradable PLGA microspheres--an alternative to incomplete Freund's adjuvant. Int J Cancer 129:407-416.

21. Silva JM, Videira M, Gaspar R, Preat V, Florindo HF Immune system targeting by biodegradable nanoparticles for cancer vaccines.

22. Mundargi RC, Babu VR, Rangaswamy V, Patel P, Aminabhavi TM Nano/micro technologies for delivering macromolecular therapeutics using poly(D,L-lactide-co-glycolide) and its derivatives.

23. Newman KD, Elamanchili P, Kwon GS, Samuel J 2002. Uptake of poly(D,L-lactic-co-glycolic acid) microspheres by antigen-presenting cells in vivo. J Biomed Mater Res 60:480-486.

24. Putney SD, Burke PA Improving protein therapeutics with sustained-release formulations.

25. Rosalia RA, Silva AL, Camps M, Allam A, Jiskoot W, van der Burg SH, Ossendorp F, Oostendorp J 2013. Efficient ex vivo induction of T cells with potent anti-tumor activity by protein antigen encapsulated in nanoparticles. Cancer Immunol Immunother.

26. Badiee A, Davies N, McDonald K, Radford K, Michiue H, Hart D, Kato M 2007. Enhanced delivery of immunoliposomes to human dendritic cells by targeting the multilectin receptor DEC-205. Vaccine 25:4757-4766.

27. Zhang XQ, Dahle CE, Baman NK, Rich N, Weiner GJ, Salem AK Potent antigen-specific immune responses stimulated by codelivery of CpG ODN and antigens in degradable microparticles.

28. Link A, Zabel F, Schnetzler Y, Titz A, Brombacher F, Bachmann MF 2012. Innate immunity mediates follicular transport of particulate but not soluble protein antigen. J Immunol 188:3724-3733.

29. Manolova V, Flace A, Bauer M, Schwarz K, Saudan P, Bachmann MF 2008. Nanoparticles target distinct dendritic cell populations according to their size. Eur J Immunol 38:1404-1413.

30. Simon LC, Sabliov CM 2013. The effect of nanoparticle properties, detection method, delivery route and animal model on poly(lactic-co-glycolic) acid nanoparticles biodistribution in mice and rats. Drug Metab Rev.

31. Jain S, O'Hagan DT, Singh M The long-term potential of biodegradable poly(lactide-co-glycolide) microparticles as the next-generation vaccine adjuvant.

32. Oyewumi MO, Kumar A, Cui Z Nano-microparticles as immune adjuvants: correlating particle sizes and the resultant immune responses.

33. Kreutz M, Tacken PJ, Figdor CG 2013. Targeting dendritic cells: why bother? Blood.

34. Schliehe C, Redaelli C, Engelhardt S, Fehlings M, Mueller M, van RN, Thiry M, Hildner K, Weller H, Groettrup M 2011. CD8- dendritic cells and macrophages cross-present poly(D,L-lactate-co-glycolate) acid microsphere-encapsulated antigen in vivo. J Immunol 187:2112-2121.

35. Johansen P, Storni T, Rettig L, Qiu Z, Der-Sarkissian A, Smith KA, Manolova V, Lang KS, Senti G, Mullhaupt B, Gerlach T, Speck RF, Bot A, Kundig TM 2008. Antigen kinetics determines immune reactivity. Proc Natl Acad Sci U S A 105:5189-5194.

36. Joshi VB, Geary SM, Salem AK 2013. Biodegradable particles as vaccine delivery systems: size matters. AAPS J 15:85-94.

37. Fifis T, Gamvrellis A, Crimeen-Irwin B, Pietersz GA, Li J, Mottram PL, McKenzie IF, Plebanski M 2004. Size-dependent immunogenicity: therapeutic and protective properties of nano-vaccines against tumors. J Immunol 173:3148-3154.

38. Gutierro I, Hernandez RM, Igartua M, Gascon AR, Pedraz JL 2002. Size dependent immune response after subcutaneous, oral and intranasal administration of BSA loaded nanospheres. Vaccine 21:67-77.

39. Silva AL, Rosalia RA, Sazak A, Carstens MG, Ossendorp F, Oostendorp J, Jiskoot W 2013. Optimization of encapsulation of a synthetic long peptide in PLGA nanoparticles: low-burst release is crucial for efficient CD8(+) T cell activation. Eur J Pharm Biopharm 83:338-345.

40. Tran KK, Shen H 2009. The role of phagosomal pH on the size-dependent efficiency of cross-presentation by dendritic cells. Biomaterials 30:1356-1362.

41. Shen H, Ackerman AL, Cody V, Giodini A, Hinson ER, Cresswell P, Edelson RL, Saltzman WM, Hanlon DJ 2006. Enhanced and prolonged cross-presentation following endosomal escape of exogenous antigens encapsulated in biodegradable nanoparticles. Immunology 117:78-88.

42. Winzler C, Rovere P, Rescigno M, Granucci F, Penna G, Adorini L, Zimmermann VS, Davoust J, Ricciardi-Castagnoli P 1997. Maturation stages of mouse dendritic cells in growth factor-dependent long-term cultures. J Exp Med 185:317-328.

43. Schuurhuis DH, Ioan-Facsinay A, Nagelkerken B, van Schip JJ, Sedlik C, Melief CJ, Verbeek JS, Ossendorp F 2002. Antigen-antibody immune complexes empower dendritic cells to efficiently prime specific CD8+ CTL responses in vivo. J Immunol 168:2240-2246.

44. Sanderson S, Shastri N 1994. LacZ inducible, antigen/MHC-specific T cell hybrids. Int Immunol 6:369-376.

45. Moore MW, Carbone FR, Bevan MJ 1988. Introduction of soluble protein into the class I pathway of antigen processing and presentation. Cell 54:777-785.

46. Sah H 1997. A new strategy to determine the actual protein content of poly(lactide-co-glycolide) microspheres. J Pharm Sci 86:1315-1318.

47. Rogo+íi-ç M, Mencer HJ, Gomzi Z 1996. Polydispersity index and molecular weight distributions of polymers. European Polymer Journal 32:1337-1344.

48. Khan S, Bijker MS, Weterings JJ, Tanke HJ, Adema GJ, van HT, Drijfhout JW, Melief CJ, Overkleeft HS, van der Marel GA, Filippov DV, van der Burg SH, Ossendorp F 2007. Distinct uptake mechanisms but similar intracellular processing of two different toll-like receptor ligand-peptide conjugates in dendritic cells. J Biol Chem 282:21145-21159.

49. Braun M, Jandus C, Maurer P, Hammann-Haenni A, Schwarz K, Bachmann MF, Speiser DE, Romero P 2012. Virus-like particles induce robust human T-helper cell responses. Eur J Immunol 42:330-340.

50. Tacken PJ, Zeelenberg IS, Cruz LJ, van Hout-Kuijer MA, van de Glind G, Fokkink RG, Lambeck AJ, Figdor CG 2011. Targeted delivery of TLR ligands to human and mouse dendritic cells strongly enhances adjuvanticity. Blood 118:6836-6844.

51. O'Hagan DT, Singh M Microparticles as vaccine adjuvants and delivery systems.

52. Mottram PL, Leong D, Crimeen-Irwin B, Gloster S, Xiang SD, Meanger J, Ghildyal R, Vardaxis N, Plebanski M Type 1 and 2 immunity following vaccination is influenced by nanoparticle size: formulation of a model vaccine for respiratory syncytial virus.

53. Xiang SD, Scholzen A, Minigo G, David C, Apostolopoulos V, Mottram PL, Plebanski M Pathogen recognition and development of particulate vaccines: does size matter?

54. Mata E, Igartua M, Hernandez RM, Rosas JE, Patarroyo ME, Pedraz JL Comparison of the adjuvanticity of two different delivery systems on the induction of humoral and cellular responses to synthetic peptides.

55. van de Weert M, van 't Hof R, van der Weerd J, Heeren RM, Posthuma G, Hennink WE, Crommelin DJ Lysozyme distribution and conformation in a biodegradable polymer matrix as determined by FTIR techniques.

56. Yeo Y, Park K Control of encapsulation efficiency and initial burst in polymeric microparticle systems.

57. Zhang Y, Zale S, Sawyer L, Bernstein H Effects of metal salts on poly(DL-lactide-co-glycolide) polymer hydrolysis.

58. Leelarasamee N, Howard SA, Malanga CJ, Luzzi LA, Hogan TF, Kandzari SJ, Ma JK Kinetics of drug release from polylactic acid-hydrocortisone microcapsules.

59. Mansour HM, Sohn M, Al-Ghananeem A, Deluca PP Materials for pharmaceutical dosage forms: molecular pharmaceutics and controlled release drug delivery aspects.

60. Cruz LJ, Tacken PJ, Fokkink R, Joosten B, Stuart MC, Albericio F, Torensma R, Figdor CG 2010. Targeted PLGA nano- but not microparticles specifically deliver antigen to human dendritic cells via DC-SIGN in vitro. J Control Release 144:118-126.

61. Pulendran B, Ahmed R 2011. Immunological mechanisms of vaccination. Nat Immunol 12:509-517.

62. Krishnamachari Y, Salem AK Innovative strategies for co-delivering antigens and CpG oligonucleotides.

63. Slutter B, Plapied L, Fievez V, Sande MA, des Rieux A, Schneider YJ, Van Riet E, Jiskoot W, Preat V Mechanistic study of the adjuvant effect of biodegradable nanoparticles in mucosal vaccination.

64. Joshi VB, Geary SM, Salem AK 2013. Biodegradable particles as vaccine delivery systems: size matters. AAPS J 15:85-94.

65. Kasturi SP, Skountzou I, Albrecht RA, Koutsonanos D, Hua T, Nakaya HI, Ravindran R, Stewart S, Alam M, Kwissa M, Villinger F, Murthy N, Steel J, Jacob J, Hogan RJ, Garcia-Sastre A, Compans R, Pulendran B 2011. Programming the magnitude and persistence of antibody responses with innate immunity. Nature 470:543-547.

66. Eckl-Dorna J, Batista FD 2009. BCR-mediated uptake of antigen linked to TLR9 ligand stimulates B-cell proliferation and antigen-specific plasma cell formation. Blood 113:3969-3977.

Supporting Information

Supporting Information Table S6.1 Distribution of MP diameters (µm) determined before (BF) and after filtration (AF) in terms of % of total particle numbers and of total particle volume. Mean diameter values calculated using the PAMAS PMA software are presented in the last row

	% Number		% Volume	
Diameter (µm)	BF	AF	BF	AF
1–2	33.2 ± 6.7	39.0 ± 11.0	0.0 ± 0.0	0.0 ± 0.0
2–5	38.6 ± 7.1	16.9 ± 2.9	0.5 ± 0.3	0.0 ± 0.0
5–10	21.2 ± 3.0	10.5 ± 5.4	2.4 ± 1.4	0.1 ± 0.1
10–15	3.7 ± 2.1	4.3 ± 3.2	1.7 ± 1.2	0.1 ± 0.1
15–20	1.3 ± 1.0	4.0 ± 3.1	1.4 ± 1.1	0.4 ± 0.3
20–25	0.6 ± 0.6	4.1 ± 2.7	1.1 ± 0.8	0.8 ± 0.7
25–30	0.3 ± 0.4	3.2 ± 1.7	1.2 ± 0.9	1.2 ± 0.9
30–40	0.4 ± 0.5	4.8 ± 0.1	2.3 ± 1.4	3.2 ± 2.1
40–50	0.2 ± 0.2	3.4 ± 0.6	2.7 ± 0.9	5.0 ± 3.5
50–60	0.1 ± 0.1	2.4 ± 0.3	2.5 ± 1.4	5.9 ± 3.8
60–75	0.1 ± 0.1	2.2 ± 0.3	6.0 ± 1.9	10.6 ± 7.6
75–100	0.2 ± 0.2	2.4 ± 1.2	17.1 ± 3.7	19.3 ± 8.5
100–125	0.1 ± 0.1	1.4 ± 1.5	20.4 ± 4.3	15.3 ± 2.7
125–150	0.0 ± 0.0	0.6 ± 0.8	11.8 ± 5.7	10.0 ± 5.9
150–200	0.0 ± 0.0	0.8 ± 1.1	29.0 ± 17.1	28.2 ± 18.1
Mean diameter	5 ± 1.0	17 ± 5.0	114 ± 16.0	112 ± 26.0

Supporting Information Table S6.2 OVA concentration sampled on the last day (day 30) of the release study. OVA concentration in supernatant (SN) was quantifed by BCA assay and by fluorescence expressed as % of total encapsulated OV

Particles	BCA Assay (% in SN)	Fluorescence (% in SN)
PLGA 50:50 NP	82 ± 14	85 ±14
PLGA 75:25 NP	53 ± 10	52 ± 9
PLGA 50:50 MP	48 ± 10	40 ± 3

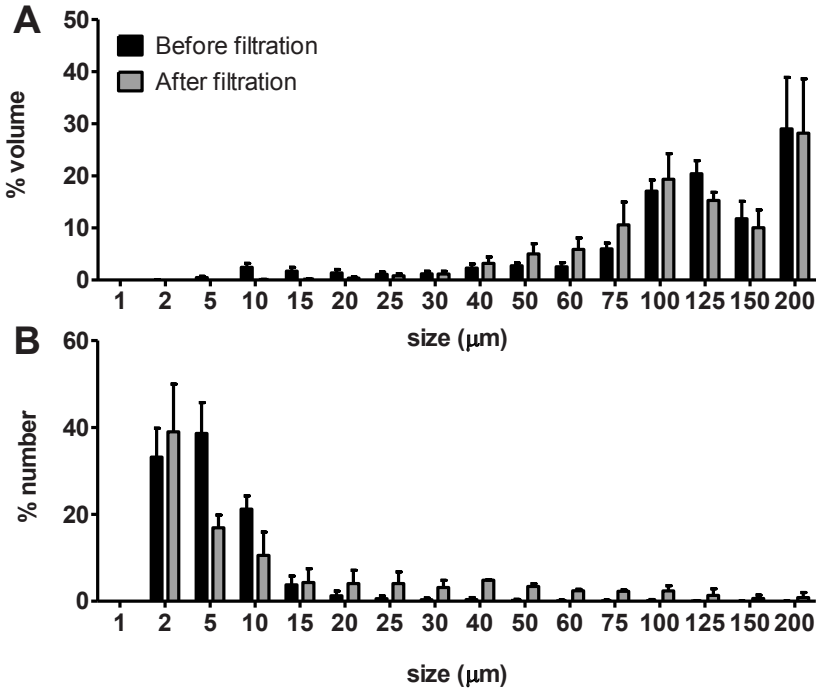

Supporting Information Figure S6.1 Size distribution of MP before filtration (BF) and after filtration (AF) determined by LO.

(A) Number distribution. **(B)** Volume distribution. Data are presented as average ± standard deviation of n = 3 independent batches.

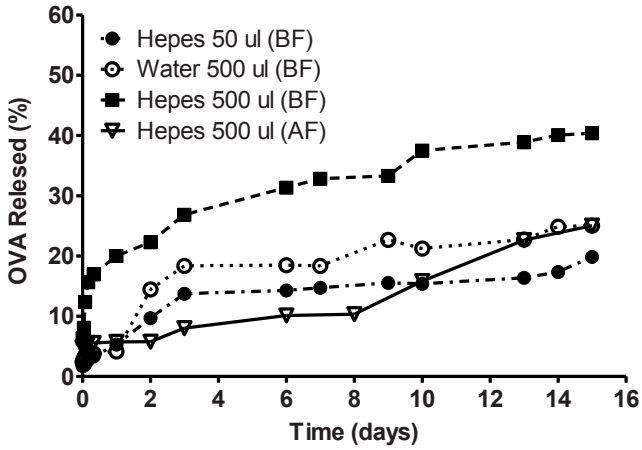

Supporting Information Figure S6.2 OVA release after filtration (AF) and before filtration (BF) of MP with different inner phase composition using PLGA 50:50 observed for 15 days. Hepes 50 µl (BF) (open diamonds) corresponds to an inner phase of 50 µl of 20 mg/ml OVA solution in 25 mM Hepes pH 7.4; and Water 500 µl (BF) (open triangles) to an inner phase of 500 µl of 2 mg/ml OVA in water. Hepes 500 µl (BF) (closed squares) and Hepes 500 µl (AF) (closed circles) correspond to an inner phase of 500 µl of 2 mg/ml OVA in 25 mM Hepes pH 7.4, before and after stirred-cell filtration, respectively.

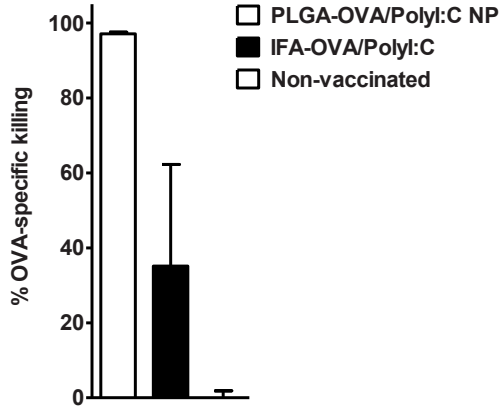

Supporting Information Figure S6.3 PLGA-OVA/poly(I:C) NP induce cytotoxic CD8$^+$ T cells *in vivo*.

In vivo cytotoxic capacity of primed OVA-specific T cells were determined in animals which received a single s.c. vaccinations with the 50 µg OVA and 20 µg poly(I:C) formulated in 50:50 PLGA-NP 50:50 or IFA. Vaccinated mice received CFSE-labeled SIINFEKL (specific) or ASNENMETM (control) short peptide loaded target cells (Ly5.1. splenocytes) 7 days after vaccination. Animals were sacrificed 18 hr later and the % target cells determined flow cytometry and calculated as described in M&M. Results shown are from one experiment and present averages ± SEM from n = 5 mice per group.